CRYSTAL GROWTH & DESIGN

pubs.acs.org/crystal

Article

Competitive Mechanochemical Solvate Formation of Theophylline in the Presence of Miscible Liquid Mixtures

Ilenia D'Abbrunzo, Martina Spadaro, Mihails Arhangelskis, Guglielmo Zingone, Dritan Hasa,* and Beatrice Perissutti*

Cite This: *Cryst. Growth Des.* 2023, 23, 8094−8102

Read Online

ACCESS | Metrics & More | Article Recommendations | Supporting Information

ABSTRACT: In this study, we investigated the mechanochemical competitive solvate formation of polymorphic Form II of theophylline in the presence of two solvate/hydrate-forming miscible liquids, namely, water and 2-pyrrolidone. It is known that theophylline transforms into a monohydrate in the presence of water, while 2-pyrrolidone gives a monosolvate or a sesquisolvate, depending on the experimental conditions. Different theophylline-to-liquid molar ratios and several water:2-pyrrolidone mixtures were used to understand the competitive formation and/or transformation between these solvates. Interconversion studies between hydrate/monosolvate/sesquisolvate forms were also conducted. The obtained results suggest that water:2-pyrrolidone mixtures have a detrimental effect on the formation of multicomponent phases, as they dramatically reduce the efficiency of incorporation of both liquids in the crystal. In fact, all milling experiments performed in the presence of water:2-pyrrolidone mixtures suggested that a higher stoichiometric ratio is needed to obtain a pure form of a specific solvate. Importantly, additional competitive milling experiments revealed a preferential inclusion of 2-pyrrolidone over water. Based on several experimental datasets performed, we conclude that the propensity of solvate formation in the presence of liquid mixtures is a consequence of a complex interplaying of physicochemical and kinetic factors.

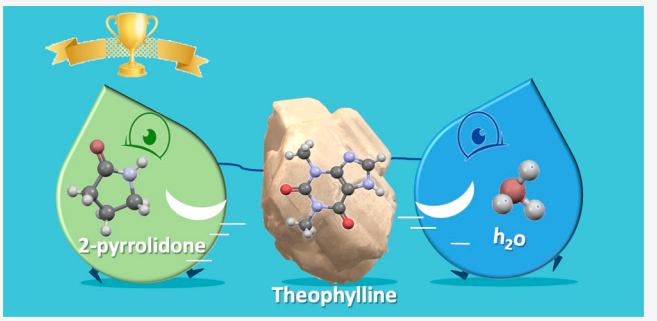

INTRODUCTION

Mechanochemistry is becoming an essential solid form screening tool in the pharmaceutical industry.[1,2] It is widely known nowadays that the control of solid form can be achieved using specific mechanochemical methods.[3−5] Specifically to multicomponent solids, mechanochemical methods have been suitably adapted for obtaining the desired crystalline form and, at the same time, improving process efficiency. In this context, there have been several reports on competitive selection of coformers for cocrystal formation.[6−9] Compared to the significant number of publications investigating the mechanochemical formation of cocrystals, studies focusing on the investigation of the selectivity of hosts for particular liquid guests using mechanochemistry, are more limited.[1,10−14] Host−guest assembly under competitive conditions is particularly interesting because the association is expected to be driven by the relatively weak non covalent interactions of hydrogen bonding, aromatic stacking, or other dispersion forces. Such screening can possibly be performed by using different mechanochemical methods.

Solvates are multicomponent solids that are often discovered serendipitously during screening for other solid forms, through purification processes (e.g., by recrystallization) or simply by storage (formation of hydrates). Importantly, there are examples of molecules in the literature, such as sulfathiazole[15] and axitinib,[16] for which solvates are almost inevitable. In such later cases, there is also a need for the development of suitable experimental conditions for obtaining neat forms. The traditional method would include desolvation rather than crystallization; however, such an approach can possibly lead to metastable polymorphs and further problems during process development. Mechanochemical desolvation through polymer-assisted grinding (POLAG) has been recently proposed as an interesting alternative to classical desolvation by heating.[17,18]

Selectivity of a solid for a particular solvent cannot be easily rationalized. Computational techniques have been employed for a mechanistic understanding and to reduce experimental work required for the discovery of new multicomponent solids. In such studies, factors such as lattice energy, solubility, interaction energy, molecular complementarity, shape and topology of the drug and the solvent, hydrogen bond

Received: July 13, 2023
Revised: September 28, 2023
Published: October 16, 2023

https://doi.org/10.1021/acs.cgd.3c00834
Cryst. Growth Des. 2023, 23, 8094−8102

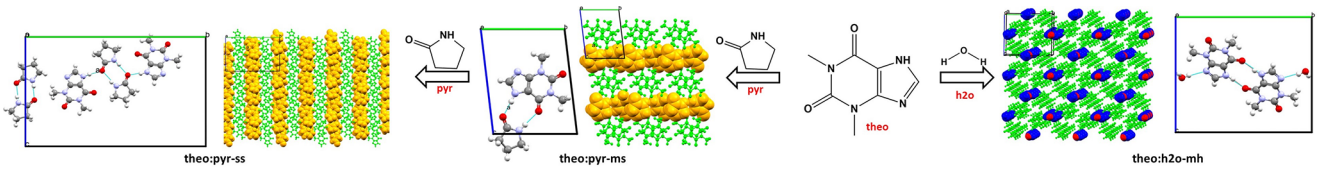

Figure 1. Crystal structures of three multicomponent forms of anhydrous theophylline (**theo**) (green) obtained in the presence of pyrrolidone (**pyr**) (yellow) [theophylline monosolvate (**theo:pyr-ms**, top left) and theophylline sesquisolvate (**theo:pyr-ss**, bottom right)] and water ($\mathbf{h_2o}$) (blue) [theophylline monohydrate (**theo:$\mathbf{h_2o}$-mh**), right].

Table 1. Overview of the Composition for Each Milling and Slurry Experiments Performed, with Indication of Water Activity (a_w) in Each Liquid Mixture

200 mg solid **theo**						300 mg solid **theo**		
1:1solid:liquid molar ratio		1:2solid:liquid molar ratio		1:3solid:liquid molar ratio		slurry bridging experiments		
$\mathbf{h_2o}$	pyr	$\mathbf{h_2o}$	pyr	$\mathbf{h_2o}$	pyr	$\mathbf{h_2o}$	pyr	a_w[a]
20 μL	0	40 μL	0	60 μL	0	5 mL		1.0125
15 μL	21 μL	30 μL	42 μL	45 μL	63.3 μL	2.08 mL	2.92 mL	0.8579
13.4 μL	27.8 μL	26.8 μL	55.6 μL	40 μL	84.4 μL	1.63 mL	3.34 mL	0.8552
10 μL	42.2 μL	20 μL	84.4 μL	30 μL	126.6 μL	0.96 mL	4.04 mL	0.8274
6.6 μL	56.5 μL	12.2 μL	113 μL	20 μL	168.8 μL	0.52 mL	4.487 mL	0.6974
5 μL	63.3 μL	10 μL	126.6 μL	15 μL	189.9 μL	0.37 mL	4.63 mL	0.5858
0	84.4 μL	0	168.8 μL	0	253.2 μL		5 mL	0.0215

[a]Calculated as proposed by ref 33.

capability[19,20] have been thoroughly investigated. These surveys, however, have been conducted mainly in the context of solution methods. Mechanochemical synthesis, on the other hand, is known to result in different chemical reactivity, different reaction pathways and different selectivity in terms of outcome of the reaction when compared to solution methods.[21,22]

In this study, a systematic exploration of the selectivity for one solvent over another of the model drug theophylline (**theo**) was performed through mechanochemistry. Additionally, the study aimed to explore the possibility of obtaining the neat form of **theo** when processed in the presence of a binary liquid mixture, where both liquids form solvates when used separately. For such purposes, two miscible solvents, namely water ($\mathbf{h_2o}$) and 2-pyrrolidone (**pyr**) were selected since they have been reported to form multicomponent solids with **theo** both in solution and through mechanochemistry.[1]

Currently, five neat polymorphs of **theo** have been reported, with polymorph II being the preferred commercial form.[23−25] Form II (indexed as BAPLOT01[26] in the Cambridge Crystallographic Database (CSD)[27]) forms a layered structure with strong hydrogen bonds and stacking interactions, with the layer-to-layer packing sustained by weaker van der Waals interactions.[1]

The monohydrate (**theo:$\mathbf{h_2o}$-mh**) has a monoclinic crystal structure, although two space groups ($P2_1$ and $P2_1/n$) and six different records have been reported in CSD.[28−31] THEOPH01 is a monoclinic channel-type hydrate, which has been shown to lose water, either at low humidity or at temperatures above 80 °C.[32,33] The dehydration process of **theo:$\mathbf{h_2o}$-mh** proceeds in two steps, namely, the dehydration and evaporation of the loosened crystal $\mathbf{h_2o}$.[34] Recently, Okeyo and coauthors[35] found a new metastable intermediate of **theo:$\mathbf{h_2o}$-mh**, during a three-step dehydration process. In **the monohydrate form**, **theo** molecules hydrogen bond to form dimers, while $\mathbf{h_2o}$ molecules form parallel channels which are cross-linked to the dimers (Figure 1) by hydrogen bonding to create layers. Literature showed that the interactions of $\mathbf{h_2o}$ with **theo** are weaker than homomeric interactions in neat crystal form II.

Two recent solvates of **theo** with **pyr**, namely, a monosolvate (**theo:pyr-ms**) and a sesquisolvate (**theo:pyr-ss**), were reported by Hasa et al.[1] and indexed in CCDC as PICMOG and PICMIA, respectively. The asymmetric unit of **theo:pyr-ms** contains one molecule of **theo** and one molecule of **pyr**, forming strong hydrogen-bonded dimers together with **theo**:**theo** stacks, which are then interlocked with each other through the stacking of **pyr** molecules (Figure 1). The asymmetric unit of the **theo:pyr-ss** structure consists of two molecules of **theo** and three molecules of **pyr**, two of these **pyr** molecules forming a homodimer, while interacting with **theo** molecules via N−H···O hydrogen bonds (Figure 1). The third **pyr** molecule forms a discrete centrosymmetric homodimer without further hydrogen-bonding interactions.

The commercial Form II of **theo** was processed mechanochemically in the presence of individual liquids ($\mathbf{h_2o}$ or **pyr**) and their mixtures. The role of different molar and volume ratios between the liquids or between the liquid mixture and solid **theo** was explored, while a series of other experimental parameters such as the milling frequency and number of milling media were kept fixed. To substantiate and evaluate the results, other parallel analyses were carried out, including measurements of grinding temperature, dissolution tests in the liquids, and **theo** wettability from single and mixed liquids. The datasets obtained from the mechanochemical screening experiments were also compared with a series of interconversion and slurry experiments. The final purpose was to understand if there is a selectivity of one guest over another among the two liquids used, and how such selectivity can be related to the properties of the two solvents, single or mixed, would affect the preferential formation of one specific multicomponent form. Additionally, we aimed to explore the experimental conditions for obtaining a neat solid in the presence of mixtures of two solvate-forming liquids.

https://doi.org/10.1021/acs.cgd.3c00834
Cryst. Growth Des. 2023, 23, 8094−8102

Rietveld refinement of the powder X-ray diffraction (PXRD) pattern was used as quantitative phase analysis to determine the relative amounts of each component in the mixtures of neat **theo**, **theo:h$_2$o-mh**, **theo:pyr-ms**, and **theo:pyr-ss**.

2. MATERIALS AND METHODS

2.1. Materials. Anhydrous **theo** Form II (≥99%) and **pyr** (≥99.0%) were purchased from Sigma−Aldrich (Milan, Italy), and used without further purification, while **h$_2$o** was freshly distilled water.

2.2. Sample Preparation. *2.2.1. Mechanochemical Processing Conditions.* A Retsch Mill MM400 (Retsch, Germany) and two stainless steel jars equipped with screw closure (internal volume of 14 mL) were used for milling experiments. The milling frequency and time were kept fixed at 25 Hz and 60 min, respectively. The grinding media consisted of two 7-mm stainless steel balls. For each mechanochemical experiment, the amount of **theo** was kept fixed at 200 mg. Different volumes of the liquid phase were added directly to the milling jars using Eppendorf Research Plus micropipettes (Eppendorf, Hamburg, Germany), as described in the following paragraphs. To ensure reproducibility, each experiment was performed in duplicate. The mechanochemical products were characterized by PXRD (see section 2.3.1) within 6 h from their preparation.

2.2.2. Composition of the Liquid Phase Added to the Milling Experiments. The first series of experiments was developed by adding to 200 mg of **theo** (approximately corresponding to 1.11×10^{-3} mol), and an *equimolar* amount of liquid, either as pure **h$_2$o** and **pyr**, or in the form of the five different **h$_2$o:pyr** mixtures reported in Table 1. The transformation of the selected molar ratios into practical volumes was performed by considering the density of the liquids at 25 °C.[36] Subsequently, two other sets of experiments were performed at **theo**:liquid molar ratios of 1:2 and 1:3, while the compositions of the liquid mixtures were the same as in the first set of experiments (Table 1).

The activity of **h$_2$o** (a_w) in each liquid mixture was calculated from the polynomial equation proposed by Zhu et al.[33] for isopropanol:**h$_2$o** mixtures as follows:

$$a_w = 0.0215 + 2.828x_w - 1.837x^2 - 2.380{x_w}^3 + 2.379{x_w}^4$$

where x_w is the mole fraction of **h$_2$o** in the liquid mixture.

An additional series of milling experiments was carried out using seven isovolumetric **h$_2$o:pyr** mixtures while maintaining constant (200 mg) the amount of solid **theo** (Table 2).

Table 2. Overview of the Liquid Composition in Isovolumetric Water:2-Pyrrolidone (h$_2$o:pyr) Mixtures for the Milling, with Indication of Solid:Liquid Ratio and the Respective Water Activity (a_w)

	200 mg solid **theo**		
	isovolumetric mixtures		
solid:liquid molar ratio	**h$_2$o**	**pyr**	a_w
1:3.1	50 μL	50 μL	0.8664
1:5.2	84.4 μL	84.4 μL	0.8659
1:6.2	100 μL	100 μL	0.8658
1:7.8	126.6 μL	126.6 μL	0.8667
1:8.7	140 μL	140 μL	0.8654
1:10.44	168.8 μL	168.8 μL	0.8682

2.2.3. Slurry Bridging Experiments. As a comparison, seven slurry experiments were performed with pure **h$_2$o**, pure **pyr**, and the same five **h$_2$o:pyr** mixtures reported in Table 1. Specifically, 5 mL of each suspension fluid and 300 mg of **theo** were transferred to a 10 mL glass vial equipped with a screw cap and sealed with parafilm. The suspensions were constantly stirred at room temperature (20 °C) for 7 days. Solid **theo** has been shown previously to be chemically stable under similar conditions.[37] Each suspension was prepared in duplicate. After 7 days, the excess solid phases were recovered and filtered by vacuum pump through a paper filter and analyzed by PXRD (see section 2.3.1).

2.2.4. Hydrate/Solvate Mechanochemical Interconversion Experiments. Preformed **theo** monohydrate (**theo:h$_2$o-mh**), **theo:pyr** monosolvate (**theo:pyr-ms**), and **theo:pyr** sesquisolvate (**theo:pyr-ss**) were used as starting materials in a series of mechanochemical interconversion experiments that are summarized in Table 3. For such purposes, the starting materials were prepared mechanochemically following the conditions reported in a previous study.[1] The obtained solid phases were characterized by PXRD. The starting materials were stored at ambient temperature in a desiccator and assayed for physical stability over a period of 3 months and before each mechanochemical interconversion experiment.

Table 3. Overview of the Mechanochemical Interconversion Experiments

	added moles of individual liquid			
starting solid (200 mg)	**h$_2$o**	**pyr**	a_w	expected outcome
theo:h$_2$o-mh (0.001 **theo** mol)		0.001 mol (76.7 μL)	0.8275	**theo:pyr-ms**
theo:h$_2$o-mh (0.001 **theo** mol)		0.0016 mol (120 μL)	0.8978	**theo:pyr-ss**
theo:pyr-ms (0.0008 **theo** mol)	0.0008 mol (13.6 μL)		0.8275	**theo:h$_2$o-mh**
theo:pyr-ss (0.0007 **theo** mol)	0.0007 mol (11.7 μL)		0.7395	**theo:h$_2$o-mh**
theo:pyr-ms (0.0008 **theo** mol)		0.0005 mol (34.4 μL)	0.0215	**theo:pyr-ss**

The interconversion milling experiments were performed by using 200 mg of preformed **theo** solvate/hydrate forms in the presence of individual liquids, as summarized in Table 3. The amount of liquid added was calculated considering the theoretical moles of anhydrous **theo** in 200 mg of solvate/hydrate inserted into the jar. Other milling conditions such as milling time, frequency, and number and size of the milling media were kept the same as in the experimental datasets mentioned above, with the only exception being that, during the interconversion experiments, the process was interrupted at 30 min and an aliquot of the solid sample was used to follow the kinetics of the process.

The same experiments were carried out also with preformed hydrate or solvate forms in the presence of equimolar or **isovolumetric** mixtures: the overviews of these trials are presented in the Supporting Information (Tables S1 and S2).

2.3. Sample Characterization and Further Analyses. *2.3.1. Powder X- Ray Diffraction.* For powder X-ray diffraction (PXRD) measurements, a Bruker D2 Phaser diffractometer (Bruker, Manheim, Germany) with a Cu Kα source (λ = 1.54 Å) was used. The system works with a 300 W low-power X-ray generator (30 kV at 10 mA). The steel sample holder used has a capacity of 300 μL, while cylindrical gearboxes in polyvinylidene fluoride (PVDF) were used for reducing the capacity to ∼100 μL of solid. In some limited cases (aliquot sampling at 30 min of grinding or in case of reduced recovery of the ground samples), a silicone-coated "zero background" sample holder was used. The conditions used for the measurement were as follows: 2θ angles from 5° to 60°, 0.02° θ increment, time step = 0.6 s.

Rietveld refinement[38] and quantitative phase analysis of the PXRD patterns was performed in TOPAS Academic 6.[39] The diffraction profile was fitted assuming the presence of four crystalline phases in the mixture: **theo**, **theo:h$_2$o-mh**, **theo:pyr-ms**, and **theo:pyr-ss**. For each phase, the peak shape parameters were modeled using a pseudo-Voigt function with simple axial divergence model. The background was modeled with a 6-term Chebyshev polynomial function. Scale factors were independently refined for each phase, and their values

https://doi.org/10.1021/acs.cgd.3c00834
Cryst. Growth Des. 2023, 23, 8094−8102

were used to determine the weight fraction of each mixture component.

Since each experiment has been repeated twice, the weight fraction of each mixture component was calculated for each experiment, and the mean of two replicates was calculated. Then, the averaged weight composition of two replicates was presented in the form of a pie chart with four different colors for four solid phases: anhydrous **theo**, **theo:h$_2$o-mh**, **theo:pyr-ms**, and **theo:pyr-ss** (as explained in the cartoon presented in Figure 2).

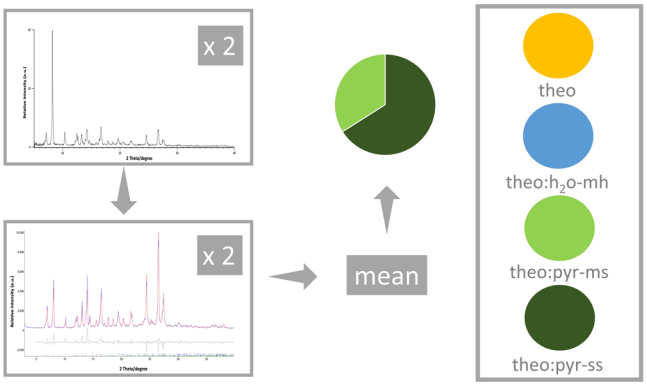

Figure 2. Cartoon explaining the meaning of the pie chart: each PXRD pattern was subjected to quantitative Rietveld refinement showing percentages of mixture components by mass: anhydrous theophylline (**theo**) (yellow), theophylline monohydrate (**theo:h$_2$o-mh**) (blue), theophylline monosolvate (**theo:pyr-ms**) (green), and theophylline sesquisolvate (**theo:pyr-ss**) (dark green). Each pattern was fitted assuming the presence of four crystalline phases in the mixture. Each pie chart represents the average composition of two replicates.

2.3.2. In Situ Measurement of Sample Temperature during Milling. The temperature inside the jar during the milling process was continuously monitored by using the ThermoJar system (InSolido Technologies j.d.o.o., Zagreb, Croatia), previously employed in the work reported by Zanolla et al.[40] The system is composed of a PMMA jar equipped with an RTD (Pt-100) thermal sensor, a wireless infrared emitter with a dedicated logging system, and software to collect, analyze, and graphic the data (LogOS). Another PMMA jar is used for balancing the weight in the milling system. The temperature measurements are conducted in the inner part of the jar, giving a description of temperature progress during milling over time. In this case, the measurements were performed every second for 60 min of grinding at 25 Hz. Using such conditions, it was possible to monitor the temperature increase during milling of 200 mg of pure **theo** in neat conditions, or in the presence of 20 μL or 84.4 μL of **h$_2$o**, while milling experiments with **pyr** could not be monitored since this liquid would damage the temperature sensor in the Thermojar system. For each experiment, four replicates were performed, and the results are reported as mean and standard deviation in the Supporting Information. The temperature differences in each experiment were analyzed statistically using the analysis of variance (ANOVA).

2.3.3. Drug Dissolution Test in the Two Solvents. Dissolution experiments were performed using 1 mg of **theo** as a solid and 50 mL of either **h$_2$o** or **pyr** as a dissolving medium, which was heated (by immersion in a water bath) with an analogous ramp to the temperature increase found during grinding. Like the milling time, the dissolution tests also lasted 60 min. The quantitative determination of dissolved **theo** was conducted every 6 s for 60 min via a spectrophotometer (Biochrom Libra S12, Biochrom, U.K., with the help of the Biochrom Data Capture software) at λ= 271 nm in **h$_2$o**[41] and λ= 274 nm in **pyr**, after suitable calibration. No solvent mixtures were used for dissolution experiments due to the difficulty in determining the concentration of **theo** in liquid mixtures. The volume withdrawn for the analysis was continuously reintroduced in the dissolution vessel to maintain a constant dissolution volume. The length of the plastic tube connected to the peristaltic pump was reduced to a minimum to avoid temperature diminution. The dissolution tests, carried out under an extractor hood, were repeated at least four times. To check statistically significant differences between the dissolution profiles conducted in **h$_2$o** and **pyr**, a Similarity Factor (f2) has been used.[42] With respect to the original FDA method, in the present study a smaller volume of the dissolution medium (50 mL) was used; profiles obtained using **h$_2$o** and **pyr** as dissolution media were compared in 10 time points (1, 2, 3, 4, 5, 6, 7, 10, 30, and 60 min). Concentration values above 85% were not

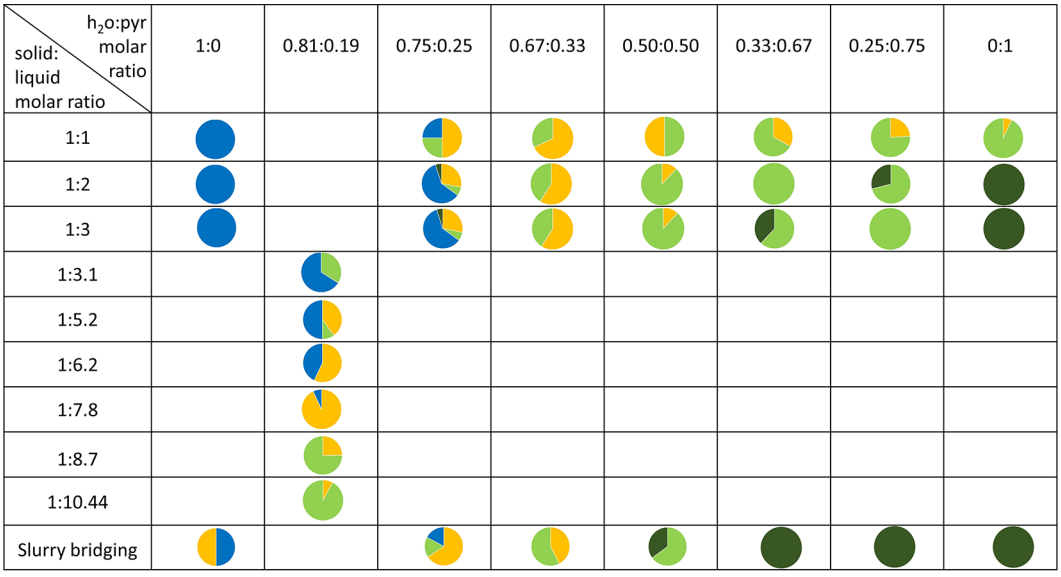

Figure 3. Solid phase recovered at the end of the grinding and slurry experiments based on anhydrous theophylline (**theo**) in the presence of individual solvents or water:2-pyrrolidone (**h$_2$o:pyr**) mixtures based on Rietveld refinement and quantitative phase analysis of the PXRD patterns. Column "0.81:0.19" corresponds to **isovolumetric h$_2$o:pyr** mixtures. Each solid phase corresponds to a different color in the pie chart: yellow represents the amount of anhydrous theophylline (**theo**), blue, green, and dark green are the amounts of the theophylline monohydrate (**theo:h$_2$o-mh**), theophylline monosolvate (**theo:pyr-ms**), and theophylline sesquisolvate (**theo:pyr-ss**), respectively.

https://doi.org/10.1021/acs.cgd.3c00834
Cryst. Growth Des. 2023, 23, 8094−8102

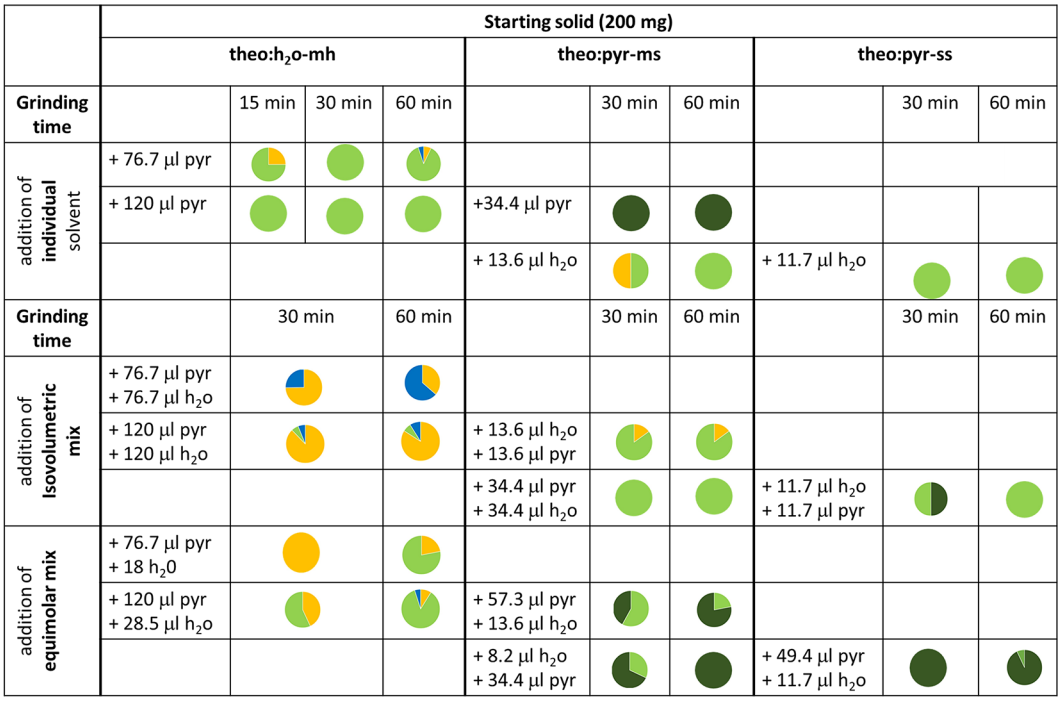

Figure 4. Solid-phase composition (weight fractions) recovered at the end of the interconversion studies starting from preformed theophylline monohydrate (**theo:h_2o-mh**), theophylline monosolvate (**theo:pyr-ms**) and theophylline sesquisolvate (**theo:pyr-ss**) phases in the presence of individual liquids or water:2-pyrrolidone (**h_2o:pyr**) mixtures. Each solid phase corresponds to a different color in the pie chart: yellow represents the amount of anhydrous theophylline (**theo**), blue, green and dark green colors indicate the amounts of the **theo:h_2o-mh**, **theo:pyr-ms**, and **theo:pyr-ss**, respectively.

considered in the comparison. Dissolution profiles were considered significantly different when f2 < 50.

2.3.4. Contact Angle. Tablets containing 250 mg of anhydrous **theo** were produced using a manual hydraulic press (Perkin-Elmer, Inc., USA) at a pressure of 1 ton per 1 min. The Drop Shape Analyzer 30E equipment (KRÜSS Scientific Drop, Inc., Germany) with Drop Shape Analysis recording software, was used for the analysis of the contact angle, an indication of the surface tension between solid **theo** and the wetting liquid. Wettability measurements were carried out using five liquid mixtures with the same composition as those reported in Table 1. Each analysis was performed in triplicate, and the contact angle was measured at both ends of the liquid drop. The differences between the averaged contact angles obtained with each liquid were statistically compared by using ANOVA.

RESULTS AND DISCUSSION

In this study, the outcome of each experiment is presented in the form of a pie chart corresponding to the average composition of two replicates. The quantification (in terms of weight fractions) of different solid phases was performed through Rietveld refinement, and each solid phase was represented with a color in the pie chart (see cartoon in Figure 2). The summary of the results of grinding and slurry experiments is reported in Figure 3, while the original patterns are reported in the Supporting Information (Figures S1−S5) and Rietveld quantification of each sample is listed in Table S3 in the Supporting Information.

From the quantitative results reported in Figure 3, several nonobvious results can be noticed. For example, in the case of milling experiments performed with different **h_2o:pyr** mixtures, the composition of the solid phase at the end of the milling experiment is not proportional to the starting molar ratio of the **h_2o:pyr** mixture. In other words, the resulting solid does not contain a stoichiometric mixture of **theo:h_2o-mh** and **theo:pyr-ms** as a function of the liquid content. Such observation is evident by following the **theo:h_2o-mh** content as a_w decreases: although only 0.25 mol of **h_2o** are required for the formation of **theo:h_2o-mh**, the hydrate is not present in any of the solid products prepared in the presence of liquid mixtures with a_w< 0.85.

A similar trend is also visible when the liquid amount over the solid increases (Figure 3): when the **h_2o:pyr** molar ratio is lower than 0.75:0.25, **theo:h_2o-mh** is no longer obtained. Interestingly, the presence of pristine **theo** after 60 min of milling is also non-negligible at higher amounts of liquid, especially when a_w > 0.80. Another observation is that the higher stoichiometry **theo:pyr-ss** appears only after all anhydrous **theo** has been previously converted in **theo:pyr-ms**, as observed by Hasa et al.[1] The results reported in Figure 3 suggest that, in the case of liquid mixtures, an amount of liquid higher than its stoichiometry is needed to obtain a specific multicomponent phase. Such an observation can be related to the strong association between **h_2o** and **pyr** molecules in the liquid mixtures. Indeed, it is known from literature that **pyr** molecules develop energetically favorable heterocomplexes with **h_2o**.[43] The interaction between these two molecules is clearly favored through the formation of hydrogen bonds, which can result in complex fluid structures. In water-dominated **h_2o:pyr** mixtures, the presence of **h_2o** molecules exerts a strong effect on the structure of fluids, decreasing the population of **pyr** dimers to an efficient development of liquid heterostructures.[43] Such a strong interaction between the two liquids can lead to a significant modification of the amounts necessary for producing pure solvates. A direct consequence of the liquid interaction is that the stability of the phases can be completely different and cannot be explained simply by considering their activity in the mixture.

https://doi.org/10.1021/acs.cgd.3c00834
Cryst. Growth Des. 2023, 23, 8094−8102

A series of slurry experiments using the same molar ratios between **h$_2$o** and **pyr** were performed for comparison (Table 1). The results, summarized in Figure 3, in the row labeled "slurry" (original PXRD patterns are depicted in Figure S4 in the Supporting Information), suggest that **theo:h$_2$o-mh** is more difficult to obtain as a pure phase, even after 7 days of slurry. It is also remarkable that the addition of only 0.25 mol of **pyr** creates more favorable conditions for the stabilization of anhydrous **theo**. In fact, after 7 days of slurry, the amount of anhydrous **theo** increases from 50% with pure water to 66% when a 0.75:0.25 mol **h$_2$o:pyr** mixture is used. On the other hand, pure **theo:pyr-ss** is obtained at $a_w < 0.70$.

In the aforementioned milling experiments, the volume of **h$_2$o** added is always lower than that of **pyr**, because of the different densities of the two liquids (see solvent parameters reported in the Supporting Information (Table S4). In order to see if this could affect the outcome of the mechanochemical reaction, another series of milling experiments were performed using **isovolumetric h$_2$o:pyr** mixtures (see Table 2). The composition of the solid product obtained after 60 min of milling is always reported in Figure 3, third column (0.81:0.19 **h$_2$o:pyr** molar ratio), while the experimental PXRD pattern are reported in Figure S5 in the Supporting Information. In such series, the value of a_w is constant (0.87), given the isovolumetric proportion of the two solvents. The results reported in Figure 3 confirm the fact that the two liquids, when used in a mixture, show a lower propensity to form a hydrated crystal/solvated crystal and a higher amount of liquid mixture then is needed to form a multicomponent phase. In the specific case, the number of moles necessary for obtaining a pure solvated phase is almost double compared to the amount of pure liquid necessary for producing a phase pure solvate. For example, the number of moles needed for getting **theo** monohydrate or monosolvate is at least double that of the pure liquids. As a result, anhydrous **theo** is the most frequent solid phase obtained from this dataset, while the highest stoichiometric solvate, i.e., **−theo:pyr-ss−** did not form, even at the 1:10.44 solid:liquid molar ratio.

Interconversion milling experiments (see Table 3 for sample composition and Figure 4 for results) were performed using preformed **theo:h$_2$o-mh**, **theo:pyr-ms**, or **theo:pyr-ss** in the presence of individual liquid or liquid mixtures. Interestingly, preformed **theo:h$_2$o-mh** converted to **theo:pyr-ms** in the presence of liquid **pyr**, while the opposite (transformation of **theo:pyr-ms** into **theo:pyr-mh** in the presence of liquid **h$_2$o**) did not occur (Figure 4). As expected, the addition of **pyr** to preformed **theo:pyr-ms** allowed the solvate stoichiometry to increase, passing to **theo:pyr-ss**, and confirming the results of the previous work.[1] On the other hand, milling preformed **theo:pyr-ss** in the presence of liquid **h$_2$o** leads to a reduction of stoichiometry, giving **theo:pyr-ms**.

These results strongly suggest a higher likelihood of **theo** to form **pyr** solvates than a hydrate. Additionally, the interconversion experiments confirmed a high interaction between **h$_2$o** and **pyr**, since processing **theo:pyr-ss** in the presence of **h$_2$o** leads to the solid losing **pyr** molecules, thus forming a solvate with a lower stoichiometry.

Analogous mechanochemical experiments were performed with **theo:h$_2$o-mh** or **theo:pyr-ms** or **theo:pyr-ss** in the presence of equimolar and isovolumetric liquid mixtures (also reported in Figure 4). When mixtures are added to the preformed solids, displacement of **h$_2$o** from **theo:pyr-ms** occurs through the formation of anhydrous **theo** as an intermediate. Interestingly, although we did not perform in situ milling experiments, the ex situ studies (the last two columns in Figure 4) suggested that when a preformed solvate or hydrate is processed in the presence of a liquid mixture, a significantly higher amount of "free" liquid is necessary to displace the crystallized solvent. Importantly, the interconversion experiments performed by using isovolumetric liquid mixtures suggest that crystallized **h$_2$o** can be displaced and replaced with **pyr**, while the opposite phenomenon was not possible under the experimental conditions used.

In the second part of the research, the mechanochemical results were assessed by considering some physicochemical characteristics of the two solvate-forming liquids used. A summary of such parameters is reported in Table S4 in the ESI. A series of physicochemical characteristics of the two liquids including the density, boiling point and the equilibrium solubility of **theo** in the specific liquid were obtained from the literature,[36,44] while other parameters such as wettability and dissolution rate of **theo** in the selected liquids were obtained experimentally.

Pure **pyr** has a higher density (1.12 g/cm^3) compared to that of **h$_2$o**, which explains the predominance of **pyr** volume in liquid mixtures. Such a difference could explain the higher propensity of **theo** to give **pyr** solvates. However, milling experiments performed by using isovolumetric mixtures (i.e., in the presence of a significantly higher amount of **h$_2$o**) did not drastically change the tendency of obtaining **pyr** solvate as a predominant phase.

Liquid volatility and the temperature increase during mechanochemical experiments were also considered as factors influencing the outcome of the mechanochemical experiments performed in this study. Our hypothesis was that, during a mechanochemical exchange experiment, the solvent that evaporates more rapidly should show a lower propensity to form a solvated solid. In-situ monitoring of the temperature within the milling jar, however, indicated that the milling temperature reached, using current operating conditions when **theo** is processed under neat conditions or in the presence of **h$_2$o**, did not exceed 35 °C (Figure S6). Therefore, the temperature reached over 60 min of milling was well below the evaporation value of both liquids and thus cannot be a key parameter for the preferential formation of **pyr** solvate.

The two liquids selected in this study differ also in their melting points. According to the study of Cruz-Cabeza et al.,[45] who have investigated the effect of entropy cost on the solvate formation by solution methods, the lower the melting point of the solvent, the higher the entropy cost would be for solvate formation. Additionally, in that study, the authors reported that increasing the operating temperature can increase the entropy cost. It means that stabilizing a liquid ingredient inside a solid would be easier for a solvent that melts at higher temperature than the operating temperature. Based on this hypothesis, the formation of **pyr** solvates is favored compared to **theo:pyr-h$_2$o** since pure **pyr** has a melting point at 25 °C (see Table S4). However, to critically contemplate the mechanochemical results observed in this study, it is needed to appropriately consider the mixing energies of the two liquids to estimate the change in the Gibbs energy from individual solvents to their mixtures, thus giving a better understanding of whether the formation of a solid phase is favored or not.

We tried to find a relation between the dissolution or solubility **in the selected liquids and their mixtures** and the preferential solvate formation by mechanochemistry but to no

https://doi.org/10.1021/acs.cgd.3c00834
Cryst. Growth Des. 2023, 23, 8094−8102

avail. In particular, variable-temperature dissolution tests (the temperature during the test was dynamically varied from 22 to 35 °C to mimic the range observed during milling experiments) were performed. Each dissolution test lasted 60 min, and sink conditions were chosen to avoid precipitation of solvated/hydrated forms at concentrations above saturation. The results reported in Figure S7 in the Supporting Information indicate a significantly different **theo** dissolution profile in $\mathbf{h_2o}$ compared to **pry.** Indeed, **theo** dissolves faster in $\mathbf{h_2o}$ than in **pyr** (after in 60 min 81% dissolved drug in $\mathbf{h_2o}$ against 63% in **pyr**). The dissolution profiles were also statistically compared by means of the similarity factor, f2, (see the Supporting Information) and the results confirmed that **theo** dissolution kinetics in the two liquids are statistically different. Such results therefore attest that the mechanochemical preferential **pyr** solvate formation, compared to the hydrate, cannot be linked to better solubilization kinetics in such liquids.

An additional possibility, given the low amount of liquid compared to the solid in the reaction mixture, is to consider the surface interfacial forces, and therefore to consider wetting capabilities of the two liquids toward solid **theo**. Despite the different superficial tensions of the two liquids,[46] the contact angle measurements (reported in Figure 5) showed an

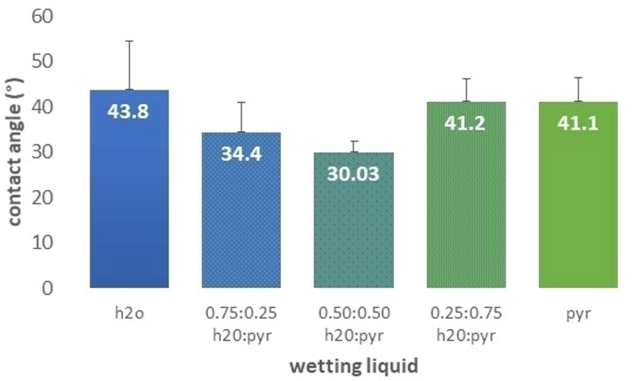

Figure 5. Anhydrous theophylline (**theo**) contact angle values with different liquids (mean ± s.d., $n = 3$).

excellent **theo** wettability by both individual solvents and their mixtures. Indeed, even if the $\mathbf{h_2o}$ surface tension is decreased in mixture with **pyr**, the difference between the averaged wetting capability of all liquids is not big enough to be statistically significant ($p > 0.05$) and there is no significant difference between the means of any pair. Therefore, the wetting capability has certainly contributed to speed up the mechanochemical process, but it is not a discriminating factor for the formation of **pyr** solvate rather than hydrate.

Finally, the reason for the propensity for the formation of **theo** solvates was also studied in light of the stability of theophylline forms. This behavior cannot be attributed to the physical stability of the monosolvate as compared to the monohydrate, since the latter has proved to be far superior from our experimental evidence (see Figures S8−S10 in the Supporting Information).

CONCLUSIONS

Although the number of studies addressing the competitive effect of binary liquid mixtures on the formation of solvates/hydrates is extremely low, the experimental evidence of this research thus cannot be compared with previous studies; some interesting conclusions can be drawn. Once again, the mechanochemical process is established as an efficient screening methodology for solid forms, as well as for solvates and hydrates. Importantly, there is a strong "competitive effect" of miscible liquids when used in combination in mechanochemical reactions. This effect is likely related to the remarkable existing interactions between the two miscible liquids, which can be favored, with respect to the interactions of singular liquids with the solid. In fact, in the case of liquid mixtures, to obtain a specific phase pure solvate, more liquid than the pure solid-to-solvent stoichiometric ratio is required. As a confirmation of $\mathbf{h_2o}$**:pyr** interactions in mixture, in interconversion studies upon grinding, there was no direct conversion from the hydrate to the solvate but an intermediate step where **theo** is in an anhydrous form. A greater propensity of **theo** to form **pyr** solvates than to form a hydrate has emerged. Once again, interconversion grinding experiments confirmed that the solvated forms prevail over the hydrate, as the preformed hydrate converts in the presence of **pyr** into monosolvate, while the opposite did not occur. Since the singular responsibility for a series of physicochemical properties of the two liquids (e.g., interfacial tension, boiling temperature, dissolution rate of theophylline in solvents, water activity, density and viscosity) has been excluded, the preferential solvate formation likely to be affected from an interplay of several factors. Further analysis and studies will be necessary (also considering mixing interactions) to describe and more comprehensively understand the process of the formation of solvates and hydrates in the presence of miscible liquid additives.

Screening experiments where the replacement of a given solvate molecule can be deliberately stimulated are potentially relevant to many areas, including pharmaceutical, where several steps of the manufacturing stages involve the use of water and/or other safe solvents. Competitive solvate experiments can be important for processing molecules that form isostructural solvates such as the case of droperidol.[10] We also believe that such types of solid-state experiments can be useful for producing innovative inclusion complexes and/or for understanding their stability in the presence of competitor molecules. Indeed, with the guidelines for the construction of inclusion compounds already established, mechanochemistry becomes particularly appealing,[47] and competitive experiments an important tool to understand their solid-state features. In this context, it is also important to highlight that, due to the development of electron diffraction methods,[48] it is nowadays possible to obtain structural characterization of pristine solids directly after mechanochemical processing.[49]

ASSOCIATED CONTENT

Supporting Information

The Supporting Information is available free of charge at https://pubs.acs.org/doi/10.1021/acs.cgd.3c00834..

PXRD pattern of 1:1, 1:2, and 1:3 solid:liquid (molar ratio) sets, slurry bridging experiments and series 2 (isovolumetric mixtures), compared to theophylline pure solid phases; temperature profiles upon grinding; theophylline dissolution profiles in different media; PXRD pattern of theophylline pure solid phases on aging; overview of the interconversion experiments with 200 mg preformed hydrate or solvate forms in the

https://doi.org/10.1021/acs.cgd.3c00834
Cryst. Growth Des. 2023, 23, 8094−8102

presence of equimolar mixtures of solvents and in the presence of isovolumetric mixtures of solvents; overview of Rietveld refinement results for each experiment performed in this study; solvent physicochemical parameters (PDF)

AUTHOR INFORMATION

Corresponding Authors

Beatrice Perissutti − *Department of Chemical and Pharmaceutical Sciences, University of Trieste p.le Europa 1, 34127 Trieste, Italy;* orcid.org/0000-0002-5766-4014; Email: bperissutti@units.it

Dritan Hasa − *Department of Chemical and Pharmaceutical Sciences, University of Trieste p.le Europa 1, 34127 Trieste, Italy;* orcid.org/0000-0003-2147-9121; Email: dhasa@units.it

Authors

Ilenia D'Abbrunzo − *Department of Chemical and Pharmaceutical Sciences, University of Trieste p.le Europa 1, 34127 Trieste, Italy*

Martina Spadaro − *Department of Chemical and Pharmaceutical Sciences, University of Trieste p.le Europa 1, 34127 Trieste, Italy*

Mihails Arhangelskis − *Faculty of Chemistry, University of Warsaw, 02-093 Warsaw, Poland;* orcid.org/0000-0003-1150-3108

Guglielmo Zingone − *Department of Chemical and Pharmaceutical Sciences, University of Trieste p.le Europa 1, 34127 Trieste, Italy;* orcid.org/0000-0003-2025-959X

Complete contact information is available at: https://pubs.acs.org/10.1021/acs.cgd.3c00834

Author Contributions

I.D., M.S., N.D., and G.Z. performed mechanochemical experiments and physicochemical characterizations. M.H. performed Rietveld refinement and quantitative phase analysis of the PXRD patterns. I.D., M.S., G.Z., and M.H. provided useful discussion on the analysis and interpretation. B.P. provided project resources and performed project administration. D.H. and B.P. conceptualized and supervised the work. D.H. and B.P. wrote the paper with review and input from all other authors.

Funding

M.A. would like to acknowledge the support of National Science Center of Poland, via the OPUS Grant No. 2020/37/B/ST5/02638.

Notes

The authors declare no competing financial interest.

ACKNOWLEDGMENTS

The authors thank Tatiana Da Ros and Erica Franceschinis for their precious cooperation.

REFERENCES

(1) Hasa, D.; Pastore, M.; Arhangelskis, M.; Gabriele, B.; Cruz-Cabeza, A. J.; Rauber, G. S.; Bond, A. D.; Jones, W. On the Kinetics of Solvate Formation through Mechanochemistry. *CrystEngComm* **2019**, *21* (13), 2097−2104.

(2) Hasa, D.; Jones, W. Screening for New Pharmaceutical Solid Forms Using Mechanochemistry: A Practical Guide. *Adv. Drug Delivery Rev.* **2017**, *117*, 147−161.

(3) Gonnet, L.; Borchers, T. H.; Lennox, C. B.; Vainauskas, J.; Teoh, Y.; Titi, H. M.; Barrett, C. J.; Koenig, S. G.; Nagapudi, K.; Friščić, T. The "*η*-Sweet-Spot" (Hmax) in Liquid-Assisted Mechanochemistry: Polymorph Control and the Role of a Liquid Additive as Either a Catalyst or an Inhibitor in Resonant Acoustic Mixing (RAM). *Faraday Discuss.* **2023**, *241*, 128.

(4) Kulla, H.; Becker, C.; Michalchuk, A. A. L.; Linberg, K.; Paulus, B.; Emmerling, F. Tuning the Apparent Stability of Polymorphic Cocrystals through Mechanochemistry. *Cryst. Growth Des.* **2019**, *19* (12), 7271−7279.

(5) Stolar, T.; Lukin, S.; Tireli, M.; Sović, I.; Karadeniz, B.; Kereković, I.; Matijašić, G.; Gretić, M.; Katančić, Z.; Dejanović, I.; Michiel, M. di; Halasz, I.; Užarević, K. Control of Pharmaceutical Cocrystal Polymorphism on Various Scales by Mechanochemistry: Transfer from the Laboratory Batch to the Large-Scale Extrusion Processing. *ACS Sustain. Chem. Eng.* **2019**, *7* (7), 7102−7110.

(6) Alsirawan, MHD. B.; Vangala, V. R.; Kendrick, J.; Leusen, F. J. J.; Paradkar, A. Coformer Replacement as an Indicator for Thermodynamic Instability of Cocrystals: Competitive Transformation of Caffeine:Dicarboxylic Acid. *Cryst. Growth Des.* **2016**, *16* (6), 3072−3075.

(7) Fischer, F.; Lubjuhn, D.; Greiser, S.; Rademann, K.; Emmerling, F. Supply and Demand in the Ball Mill: Competitive Cocrystal Reactions. *Cryst. Growth Des.* **2016**, *16* (10), 5843−5851.

(8) Fischer, F.; Joester, M.; Rademann, K.; Emmerling, F. Survival of the Fittest: Competitive Co-Crystal Reactions in the Ball Mill. *Chem.—Eur. J.* **2015**, *21* (42), 14969−14974.

(9) Yamamoto, K.; Tsutsumi, S.; Ikeda, Y. Establishment of Cocrystal Cocktail Grinding Method for Rational Screening of Pharmaceutical Cocrystals. *Int. J. Pharm.* **2012**, *437* (1), 162−171.

(10) Bērziņš, A.; Skarbulis, E.; Rekis, T.; Actiņš, A. On the Formation of Droperidol Solvates: Characterization of Structure and Properties. *Cryst. Growth Des.* **2014**, *14* (5), 2654−2664.

(11) Caira, M. R.; Nassimbeni, L. R.; Toda, F.; Vujovic, D. Inclusion of Aminobenzonitrile Isomers by a Diol Host Compound: Structure and Selectivity. *J. Am. Chem. Soc.* **2000**, *122* (39), 9367−9372.

(12) Friščić, T.; Halasz, I.; Strobridge, F. C.; Dinnebier, R. E.; Stein, R. S.; Fábián, L.; Curfs, C. A Rational Approach to Screen for Hydrated Forms of the Pharmaceutical Derivative Magnesium Naproxen Using Liquid-Assisted Grinding. *CrystEngComm* **2011**, *13* (9), 3125−3129.

(13) Karki, S.; Friščić, T.; Jones, W.; Motherwell, W. D. S. Screening for Pharmaceutical Cocrystal Hydrates via Neat and Liquid-Assisted Grinding. *Mol. Pharmaceutics* **2007**, *4* (3), 347−354.

(14) Zanolla, D.; Gigli, L.; Hasa, D.; Chierotti, M. R.; Arhangelskis, M.; Demitri, N.; Jones, W.; Voinovich, D.; Perissutti, B. Mechanochemical Synthesis and Physicochemical Characterization of Previously Unreported Praziquantel Solvates with 2-Pyrrolidone and Acetic Acid. *Pharmaceutics* **2021**, *13* (10), 1606.

(15) Bingham, A. L.; Hughes, D. S.; Hursthouse, M. B.; Lancaster, R. W.; Tavener, S.; Threlfall, T. L. Over One Hundred Solvates of Sulfathiazole. *Chem. Commun.* **2001**, No. 7, 603−604.

(16) Campeta, A. M.; Chekal, B. P.; Abramov, Y. A.; Meenan, P. A.; Henson, M. J.; Shi, B.; Singer, R. A.; Horspool, K. R. Development of a Targeted Polymorph Screening Approach for a Complex Polymorphic and Highly Solvating API. *J. Pharm. Sci.* **2010**, *99* (9), 3874−3886.

(17) Scaramuzza, D.; Schneider Rauber, G.; Voinovich, D.; Hasa, D. Dehydration without Heating: Use of Polymer-Assisted Grinding for Understanding the Stability of Hydrates in the Presence of Polymeric Excipients. *Cryst. Growth Des.* **2018**, *18* (9), 5245−5253.

(18) Terban, M. W.; Madhau, L.; Cruz-Cabeza, A. J.; Okeyo, P. O.; Etter, M.; Schulz, A.; Rantanen, J.; Dinnebier, R. E.; Billinge, S. J. L.; Moneghini, M.; Hasa, D. Controlling Desolvation through Polymer-Assisted Grinding. *CrystEngComm* **2022**, *24* (12), 2305−2313.

(19) Boothroyd, S.; Kerridge, A.; Broo, A.; Buttar, D.; Anwar, J. Why Do Some Molecules Form Hydrates or Solvates? *Cryst. Growth Des.* **2018**, *18* (3), 1903−1908.

(20) Loschen, C.; Klamt, A. Computational Screening of Drug Solvates. *Pharm. Res.* **2016**, *33* (11), 2794−2804.
(21) Ayoub, G.; Štrukil, V.; Fábián, L.; Mottillo, C.; Bao, H.; Murata, Y.; Moores, A.; Margetić, D.; Eckert-Maksić, M.; Friščić, T. Mechanochemistry vs. Solution Growth: Striking Differences in Bench Stability of a Cimetidine Salt Based on a Synthetic Method. *CrystEngComm* **2018**, *20* (45), 7242−7247.
(22) Lombard, J.; Laker, H.; Prins, F.; Wahl, H.; le Roex, T.; Haynes, D. A. Selectivity of Hosts for Guests by Liquid-Assisted Grinding: Differences between Solution and Mechanochemistry. *CrystEngComm* **2021**, *23* (42), 7380−7384.
(23) Eddleston, M. D.; Hejczyk, K. E.; Bithell, E. G.; Day, G. M.; Jones, W. Determination of the Crystal Structure of a New Polymorph of Theophylline. *Chem.—Eur. J.* **2013**, *19* (24), 7883−7888.
(24) Roy, C.; Vega-González, A.; Subra-Paternault, P. Theophylline Formulation by Supercritical Antisolvents. *Int. J. Pharm.* **2007**, *343* (1), 79−89.
(25) Seton, L.; Khamar, D.; Bradshaw, I. J.; Hutcheon, G. A. Solid State Forms of Theophylline: Presenting a New Anhydrous Polymorph. *Cryst. Growth Des.* **2010**, *10* (9), 3879−3886.
(26) Ebisuzaki, Y.; Boyle, P. D.; Smith, J. A. Methylxanthines. I. Anhydrous Theophylline. *Acta Crystallogr., Sect. C* **1997**, *53* (6), 777−779.
(27) Groom, C. R.; Bruno, I. J.; Lightfoot, M. P.; Ward, S. C. The Cambridge Structural Database. *Acta Crystallogr. Sect. B: Struct. Sci. Cryst. Eng. Mater.* **2016**, *72* (2), 171−179.
(28) Fucke, K.; McIntyre, G. J.; Wilkinson, C.; Henry, M.; Howard, J. A. K.; Steed, J. W. New Insights into an Old Molecule: Interaction Energies of Theophylline Crystal Forms. *Cryst. Growth Des.* **2012**, *12* (3), 1395−1401.
(29) Majodina, S.; Ndima, L.; Abosede, O. O.; Hosten, E. C.; Lorentino, C. M. A.; Frota, H. F.; Sangenito, L. S.; Branquinha, M. H.; Santos, A. L. S.; Ogunlaja, A. S. Physical Stability Enhancement and Antimicrobial Properties of a Sodium Ionic Cocrystal with Theophylline. *CrystEngComm* **2021**, *23* (2), 335−352.
(30) Sun, C.; Zhou, D.; Grant, D. J. W.; Young, V. G. J. Theophylline Monohydrate. *Acta Crystallogr., Sect. E: Struct. Rep. Online* **2002**, *58* (4), o368−o370.
(31) Sutor, D. J. The Structures of the Pyrimidines and Purines. VI. The Crystal Structure of Theophylline. *Acta Crystallogr.* **1958**, *11* (2), 83−87.
(32) Ticehurst, M. D.; Storey, R. A.; Watt, C. Application of Slurry Bridging Experiments at Controlled Water Activities to Predict the Solid-State Conversion between Anhydrous and Hydrated Forms Using Theophylline as a Model Drug. *Int. J. Pharm.* **2002**, *247* (1), 1−10.
(33) Zhu, H.; Yuen, C.; Grant, D. J. W. Influence of Water Activity in Organic Solvent + Water Mixtures on the Nature of the Crystallizing Drug Phase. 1. Theophylline. *Int. J. Pharm.* **1996**, *135* (1), 151−160.
(34) Suihko, E.; Ketolainen, J.; Poso, A.; Ahlgren, M.; Gynther, J.; Paronen, P. Dehydration of Theophylline Monohydrate—A Two Step Process. *Int. J. Pharm.* **1997**, *158* (1), 47−55.
(35) Okeyo, P. O.; Ilchenko, O.; Slipets, R.; Larsen, P. E.; Boisen, A.; Rades, T.; Rantanen, J. Imaging of Dehydration in Particulate Matter Using Raman Line-Focus Microscopy. *Sci. Rep.* **2019**, *9* (1), 7525.
(36) Lide, D. R. *Handbook of Organic Solvents*; CRC Press, 1994.
(37) Baptista, R. J.; Mitrano, F. P. Stability and Compatibility of Cimetidine Hydrochloride and Aminophylline in Dextrose 5% in Water Injection. *Drug Intell. Clin. Pharm.* **1988**, *22* (7−8), 592−593.
(38) Rietveld, H. M. Line Profiles of Neutron Powder-Diffraction Peaks for Structure Refinement. *Acta Crystallogr.* **1967**, *22* (1), 151−152.
(39) Coelho, A. A. TOPAS and TOPAS-Academic: An Optimization Program Integrating Computer Algebra and Crystallographic Objects Written in C++. *J. Appl. Crystallogr.* **2018**, *51* (1), 210−218.
(40) Zanolla, D.; Perissutti, B.; Vioglio, P. C.; Chierotti, M. R.; Gigli, L.; Demitri, N.; Passerini, N.; Albertini, B.; Franceschinis, E.; Keiser, J.; Voinovich, D. Exploring Mechanochemical Parameters Using a DoE Approach: Crystal Structure Solution from Synchrotron XRPD and Characterization of a New Praziquantel Polymorph. *Eur. J. Pharm. Sci.* **2019**, *140*, 105084.
(41) Cohen, J. L. Theophylline. In *Analytical Profiles of Drug Substances*; Florey, K., Ed.; Academic Press, 1975; Vol. *4*, pp 466−493, DOI: 10.1016/S0099-5428(08)60024-6.
(42) Food and Drug Administration. *Dissolution Testing of Immediate Release Solid Oral Dosage Forms*. U.S. Food and Drug Administration. https://www.fda.gov/regulatory-information/search-fda-guidance-documents/dissolution-testing-immediate-release-solid-oral-dosage-forms (accessed June 30, 2023).
(43) Dávila, M. J.; Alcalde, R.; Aparicio, S. Pyrrolidone Derivatives in Water Solution: An Experimental and Theoretical Perspective. *Ind. Eng. Chem. Res.* **2009**, *48* (2), 1036−1050.
(44) Bustamante, P.; Navarro-Lupión, J.; Peña, M. A.; Escalera, B. Hildebrand Solubility Parameter to Predict Drug Release from Hydroxypropyl Methylcellulose Gels. *Int. J. Pharm.* **2011**, *414* (1−2), 125−130.
(45) Cruz-Cabeza, A. J.; Wright, S. E.; Bacchi, A. On the Entropy Cost of Making Solvates. *Chem. Commun.* **2020**, *56* (38), 5127−5130.
(46) Lerk, C. F.; Lagas, M.; Boelstra, J. P.; Broersma, P. Contact Angles of Pharmaceutical Powders. *J. Pharm. Sci.* **1977**, *66* (10), 1480−1481.
(47) Friščić, T.; Trask, A. V.; Jones, W.; Motherwell, W. D. S. Screening for Inclusion Compounds and Systematic Construction of Three-Component Solids by Liquid-Assisted Grinding. *Angew. Chem., Int. Ed.* **2006**, *45* (45), 7546−7550.
(48) Karothu, D. P.; Alhaddad, Z.; Göb, C. R.; Schürmann, C. J.; Bücker, R.; Naumov, P. The Elusive Structure of Levocetirizine Dihydrochloride Determined by Electron Diffraction. *Angew. Chem., Int. Ed.* **2023**, *62* (26), No. e202303761.
(49) Gogoi, D.; Sasaki, T.; Nakane, T.; Kawamoto, A.; Hojo, H.; Kurisu, G.; Thakuria, R. Structure Elucidation of Olanzapine Molecular Salts by Combining Mechanochemistry and Micro-Electron Diffraction. *Cryst. Growth Des.* **2023**, *23* (8), 5821−5826.

https://doi.org/10.1021/acs.cgd.3c00834
Cryst. Growth Des. 2023, 23, 8094−8102